ISSN 1075-7015, Geology of Ore Deposits, 2016, Vol. 58, No. 8, pp. 653–665. © Pleiades Publishing, Ltd., 2016.
Original Russian Text © N.V. Chukanov, A.V. Kasatkin, N.V. Zubkova, S.N. Britvin, L.A. Pautov, I.V. Pekov, D.A. Varlamov, Ya.V. Bychkova, A.B. Loskutov, E.A. Novgorodova, 2016, published in Zapiski Rossiiskogo Mineralogicheskogo Obshchestva, 2016, No. 1, pp. 48–67.

NEW MINERALS, CLASSIFICATION, AND NOMENCLATURE OF MINERALS

Tatarinovite $Ca_3Al(SO_4)[B(OH)_4](OH)_6 \cdot 12H_2O$, a New Ettringite-Group Mineral from the Bazhenovskoe Deposit, Middle Urals, Russia, and Its Crystal Structure[1]

N. V. Chukanov[a, b, *], A. V. Kasatkin[c], N. V. Zubkova[b], S. N. Britvin[d], L. A. Pautov[c], I. V. Pekov[b], D. A. Varlamov[e], Ya. V. Bychkova[f], A. B. Loskutov[g], and E. A. Novgorodova[h]

[a] *Institute of Problems of Chemical Physics, Russian Academy of Sciences, Chernogolovka, Moscow oblast, 142432 Russia*
[b] *Faculty of Geology, Moscow State University, Moscow, 119991 Russia*
[c] *Fersman Mineralogical Museum of Russian Academy of Sciences, Leninsky pr. 18–2, Moscow, 119071 Russia*
[d] *Faculty of Geology, St. Petersburg State University, Universitetskaya nab. 7/9, St. Petersburg, 199034 Russia*
[e] *Institute of Experimental Mineralogy, Russian Academy of Sciences, Chernogolovka, Moscow oblast, 142432 Russia*
[f] *Institute of Geology of Ore Deposits, Petrography, Mineralogy, and Geochemistry, Russian Academy of Sciences, Staromonetny per. 35, Moscow, 109017, Russia*
[g] *Ul. Voikova 62–500, Asbest, Sverdlovsk Oblast, 624266 Russia*
[h] *Ul. Voikova 67–6, Asbest, Sverdlovsk Oblast, 624266 Russia*
**e-mail: chukanov@icp.ac.ru*

Received October 13, 2015

Abstract—A new mineral, tatarinovite, ideally $Ca_3Al(SO_4)[B(OH)_4](OH)_6 \cdot 12H_2O$, has been found in cavities of rhodingites at the Bazhenovskoe chrysotile asbestos deposit, Middle Urals, Russia. It occurs (1) colorless, with vitreous luster, bipyramidal crystals up to 1 mm across in cavities within massive diopside, in association with xonotlite, clinochlore, pectolite and calcite, and (2) as white granular aggregates up to 5 mm in size on grossular with pectolite, diopside, calcite, and xonotlite. The Mohs hardness is 3; perfect cleavage on (100) is observed. $D_{meas} = 1.79(1)$, $D_{calc} = 1.777$ g/cm^3. Tatarinovite is optically uniaxial (+), $\omega = 1.475(2)$, $\varepsilon = 1.496(2)$. The IR spectrum contains characteristic bands of SO_4^{2-}, CO_3^{2-}, $B(OH)_4^-$, $B(OH)_3$, $Al(OH)_6^{3-}$, $Si(OH)_6^{2-}$, OH^-, and H_2O. The chemical composition of tatarinovite (wt %; ICP-AES; H_2O was determined by the Alimarin method; CO_2 was determined by selective sorption on askarite) is as follows: 27.40 CaO, 4.06 B_2O_3, 6.34 Al_2O_3, 0.03 Fe_2O_3, 2.43 SiO_2, 8.48 SO_3, 4.2 CO_2, 46.1 H_2O, total is 99.04. The empirical formula (calculated on the basis of 3Ca apfu) is $H_{31.41}Ca_{3.00}(Al_{0.76}Si_{0.25})_{\Sigma 1.01} \cdot (B_{0.72}S_{0.65}C_{0.59})_{\Sigma 1.96}O_{24.55}$. Tatarinovite is hexagonal, space gr. $P6_3$, $a = 11.1110(4)$ Å, $c = 10.6294(6)$ Å, $V = 1136.44(9)$ Å^3, $Z = 2$. Its crystal chemical formula is $Ca_3(Al_{0.70}Si_{0.30}) \cdot \{[SO_4]_{0.34}[B(OH)_4]_{0.33}[CO_3]_{0.24}\}\{[SO_4]_{0.30}[B(OH)_4]_{0.34}[CO_3]_{0.30}[B(OH)_3]_{0.06}\}(OH_{5.73}O_{0.27}) \cdot 12H_2O$. The strongest reflections of the powder X-ray diffraction pattern [d, Å (I, %) (hkl)] are 9.63 (100) (100), 5.556 (30) (110), 4.654 (14) (102), 3.841 (21) (112), 3.441 (12) (211), 2.746 (10) (302), 2.538 (12) (213). Tatarinovite was named in memory of the Russian geologist and petrologist Pavel Mikhailovich Tatarinov (1895–1976), a well-known specialist in chrysotile asbestos deposits. Type specimens have been deposited at the Fersman Mineralogical Museum of the Russian Academy of Sciences, Moscow.

Keywords: Tatarinovite, new mineral, ettringite group, boron, rhodingite, Bazhenovskoe deposit, the Middle Urals

DOI: 10.1134/S1075701516080080

INTRODUCTION

Ettringite-group minerals (EGM) are typical constituents of the latest low-temperature hydrothermal paragenetic assemblages related to high-Ca altered rocks of various geneses: skarns, metamorphosed xenoliths of carbonate rocks in mafic and alkaline lavas, rhondingites, etc. EGM are important and are frequently the major carriers of B and S in these assemblages.

Trigonal and hexagonal minerals with the general formula $Ca_6[M_2(OH,O)_{12} \cdot nH_2O]A_{2-3}$, where M = Si,

[1] A new mineral tatarinovite and its name were approved by the Commission on New Minerals, Nomenclature, and Classification of Minerals, International Mineralogical Association, August 10, 2015, IMA no. 2015-055.

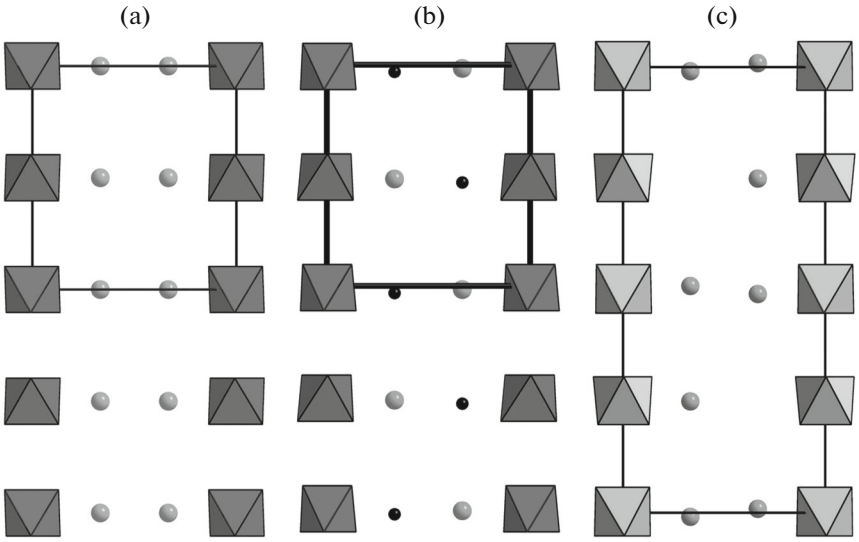

Fig. 1. Scheme of arrangement of central atoms of *A*-anions (S^{6+} –circles, C^{4+} – black dots) in structure types of (a) carraraite, space group $P6_3/m$ (kottenheimite), (b) thaumasite, space group $P6_3$, and (c) ettringite, space group $P31c$. $Si(OH)_6$ and $Al(OH)_6$ are dark and light octahedra, respectively. Drawn after Chukanov et al. (2012), Martucci and Cruciani (2006), and Moore and Taylor (1970). The unit cells are outlined.

Al, Cr^{3+}, Ge^{4+}, Fe^{3+} or Mn^{4+}; $n = 22–26$; $A = SO_4^{2-}$, CO_3^{2-}, SO_3^{2-}, PO_3OH^{2-} or $B(OH)_4^-$ belong to the ettringite group. The crystal structure of EGM is based on infinite $Ca_3[M(OH)_6(H_2O)_m]$ columns formed by $M(OH)_6$ octahedra and trimers of edge-sharing Ca-centered $Ca(OH)_4(H_2O)_x$ polyhedra, where x and the coordination of Ca depend on the total number n of H_2O molecules in the mineral formula (Skoblinskaya et al., 1975). *A* anions are located inside channels running parallel to the *c* axis. Note that a bipyramidal or less frequent short-prismatic habit is a characteristic feature of most samples of B-bearing EGM (charlesite, sturmanite, buryatite), whereas B-free minerals (ettringite, thaumasite, hielscherite, kottenheimite) usually occur as long-prismatic crystals.

The ettringite group includes minerals belonging to three related structure types. Two hexagonal EGM, namely, carraraite $Ca_3Ge(SO_4,CO_3)_2(OH)_6 \cdot 12H_2O$ (Merlino and Orlandi, 2001) and kottenheimite $Ca_3Si(SO_4)_2(OH)_6 \cdot 12H_2O$ (Chukanov et al., 2012), have disordered *A*-anions, which for this structure results in the highest possible motif space group $P6_3/m$ and small unit cell with parameter $c \approx 11$ Å (Fig. 1a). The second type also includes hexagonal members with $c \approx 11$ Å that crystallize in the space group $P6_3$: jouravskite $Ca_3Mn^{4+}(SO_4)(CO_3)(OH)_6 \cdot 12H_2O$ (Granger and Protas, 2012), thaumasite $Ca_3Si(SO_4)(CO_3)(OH)_6 \cdot 12H_2O$ (Effenberger et al., 1983; Martucci and Cruciani, 2006), hielscherite $Ca_3Si(SO_4)(SO_3)(OH)_6 \cdot 11H_2O$ (Pekov et al., 2012), imayoshiite $Ca_3Al(CO_3)[B(OH)_4](OH)_6 \cdot 12H_2O$ (Nishio-Hamane et al., 2015), and tatarinovite $Ca_3Al(SO_4)[B(OH)_4](OH)_6 \cdot 12H_2O$ discussed in this study. In their structures, intra-channel *A*-anions are ordered that causes symmetry lowering relative to $P6_3/m$ (Fig. 1b). Both structure types are characterized by the ratio Ca : *A* = 3 : 2.

The third structure type (Fig. 1c) includes trigonal (space group $P31c$) EGM, namely, ettringite $Ca_6Al_2(SO_4)_3(OH)_{12} \cdot 26H_2O$ (Moore and Taylor, 1970), sturmanite $Ca_6Fe_2^{3+}(SO_4)_2[B(OH)_4](OH)_{12} \cdot 25H_2O$ (Peacor et al., 1983; Pushcharovsky et al., 2004), charlesite $Ca_6Al_2(SO_4)_2[B(OH)_4](OH)_{12} \cdot 26H_2O$ (Dunn et al., 1983) and its unnamed analog with $CO_3 > SO_4$ (Kusachi et al., 2008). These minerals are characterized by a doubled *c* parameter and EGM stoichiometry differing from hexagonal: the ratio Ca : *A* is 2 : 1.

Bipyramidal crystals of EGM found in one of the rhodingite bodies at the Bazhenovskoe deposit were initially interesting in their morphological features, which sharply differ from those of thaumasite crystals typical of similar assemblages. Determination of the chemical composition revealed high contents of boron and aluminum in the mineral, and X-ray structure analysis showed that this EGM belongs to the structure type of thaumasite. These data allowed its treatment as a new mineral species, an analog of imayoshiite, $Ca_6Al_2(CO_3)_2[B(OH)_4]_2(OH)_{12} \cdot 24H_2O$ with SO_4^{2-} instead of CO_3^{2-}. The mineral was named in memory of the Soviet geologist and petrologist Pavel Mikhailovich Tatarinov (1895–1976), a well-known specialist of chrysotile asbestos deposits, who actively studied the Bazhenovskoe deposit. Tatarinov was also

a professor, corresponding member of the USSR Academy of Sciences, President of the USSR Mineralogical Society from 1962 to 1976, and editor-in-chief of *Zapiski Vsesoyuznogo Mineralogicheskogo Obshchestva*.

Type specimens of tatarinovite have been deposited at the Fersman Mineralogical Museum of the Russian Academy of Sciences, Moscow, with the registration numbers 4736/1 and 4736/2.

OCCURRENCE AND GENERAL DESCRIPTION

Samples of this new mineral were collected in September 2012 from a rhodingite body opened at the eastern wall of the Southern open pit at the Bazhenovskoe long-fibrous chrysotile asbestos deposit near the town of Asbest, Sverdlovsk oblast, Middle Urals, Russia. Mineralogical and petrological data for various rocks of this deposit, including rhodingites, are given in detail in certain publications (Sokolov and Luzin, 1981; Zoloev et al., 1985; *Mineralogiya* ..., 1996; Erokhin, 1997; Erokhin and Shagalov, 1998; Antonov, 2003; Efimov, 2004; Loskutov and Novgorodova, 2012). In general, Bazhenovskoe rhodingites are low-grade metamorphism products of gabbroic dikes hosted in serpentinite. Grossular, diopside, and clinochlore are the major minerals of the rock; in some cases, they contain substantial amounts of vesuvianite, clinozoisite, prehnite, serpentine, amphiboles of the tremolite–actinolite solid solution, wollastonite, and calcite. Late constituents are zeolites, apophyllite, calcite, aragonite, and diverse Ca silicates (pectolite, xonotlite, tobermorite, plombièrite, hillebrandite, jennite); rosenhahnite (Zadov et al., 2000) and recently discovered kasatkinite, $Ba_2Ca_8B_5Si_8O_{32}(OH)_3 \cdot 6H_2O$ (Pekov et al., 2013) are unique.

The steeply dipping about 70° rhodingite body of about 1.5 m in thickness, where tatarinovite has been found, is the contact zone between partly rhodingitized gabbroic dike and host serpentinite and is traced for a few hundred meters. The new mineral is the latest in two mineral assemblages.

In the first-type assemblage, which developed at the margins of the rhodingite body, separate water-transparent lenticular, flattened parallel to [001] bipyramidal crystals of tatarinovite reaching 1 mm across (average 0.5 mm) overgrowing white acicular to hair-like crystals of xonotlite are associated with lamellar crystals of clinochlore within the cavities of predominantly diopside aggregate (Figs. 2a, 2b, 3). Occasionally, tatarinovite individuals overgrow colorless long-prismatic calcite crystals up to 5 cm long. This assemblage also includes snow-white felted pectolite aggregates. Crystals of the new mineral are formed by the blunt bipyramid {104} (the main form) and prism {100} faces (usually, the only subordinate form). On some crystals, weakly developed pinacoid {001} faces are observed.

In the assemblage of the second type, observed in both the margins and central part of the rhodingite body, tatarinovite forms white massive sugarlike granular aggregates up to 5 cm in size composed of anhedral individuals and grains with elements of crystal faces overgrowing crystal crusts of pinkish orange grossular (Fig. 2c).

White spherulites of pectolite, short-prismatic crystals of pale-blue diopside, and minor calcite and xonotlite are present in this assemblage.

PHYSICAL PROPERTIES

Individuals of tatarinovite are transparent and colorless, whereas in aggregates, the mineral is white to snow-white and semitransparent or nearly opaque. The streak is white. The luster is lustrous. Under UV light the mineral is not luminescent. The cleavage is perfect parallel to (100). The Mohs' hardness is 3. The density measured by floatation in heavy liquids (mixed tribromomethane and acetone) is 1.79(1) g/cm^3; the calculated density is 1.777 g/cm^3.

Tatarinovite is optically positive, uniaxial, ω = 1.475(2), ε = 1.496(2). In thin section, the mineral is colorless and nonpleochroic.

The IR spectra of tatarinovite and other EGM powdered samples prepared as pellets pressed with KBr (Fig. 4) were measured using a Bruker ALPHA FTIR spectrometer within the wavenumber range 360–3800 cm^{-1} with a resolution of 4 cm^{-1} and of 16 scans. A pure KBr disc was used as a reference.

The wavenumbers (in cm^{-1}) and assignment of the bands in the IR spectrum of dachiardite-K are as follows (s is strong band, w is weak band, and sh is shoulder): 3614s, 3495sh, 3460sh, 3425s, 3240sh (O–H stretching vibrations of H_2O molecules and OH groups), 2420w, 2252w (O–H stretching vibrations of hydrosulfate groups HSO_4^- formed as a result of reversible proton transfer $SO_4^{2-} + H_2O \leftrightarrow HSO_4^- + OH^-$; the low intensities of these bands indicate that this dynamic chemical equilibrium is strongly shifted to the left), 1686 (bending vibrations of H_2O molecules), 1403s (asymmetric stretching vibrations of CO_3^{2-} anions), 1227w, 1195sh (asymmetric B–O stretching vibrations of $B(OH)_3$ molecules and $B(OH)_4$ anions), 1114s (asymmetric stretching vibrations of SO_4^{2-} anions), 991, 953 (mixed B–O stretching and B–O–H bending vibrations of $B(OH)_4$ anions), 879 (out of plane bending vibrations of CO_3^{2-} anions), 720sh (Si–O stretching vibrations of $Si(OH)_6$ octahedra), 675s, 645sh, 595 (bending vibrations of anions SO_4^{2-}), 555 (Al–O stretching vibrations of $Al(OH)_6$


(a)

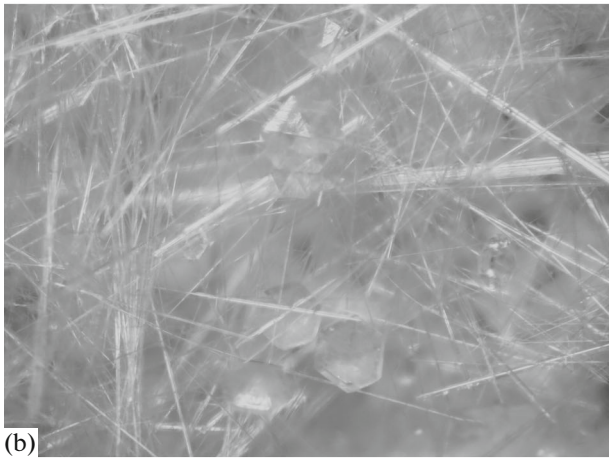
(b)

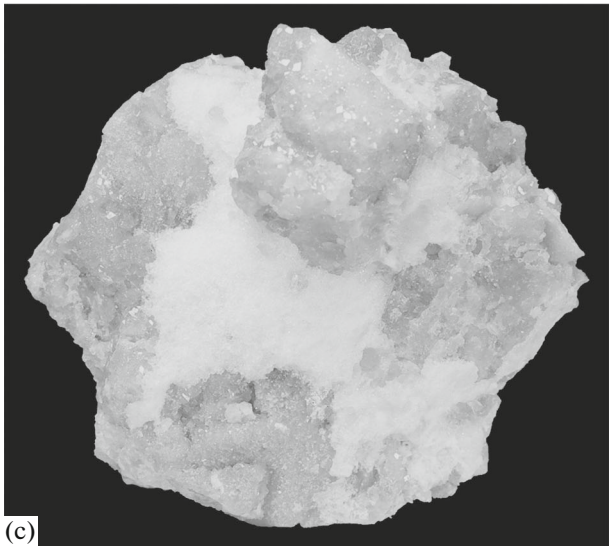
(c)

Fig. 2. (a) Colorless bipyramidal crystals of tatarinovite with white acicular xonotlite, clinochlore (dark zones), and coarse-crystalline calcite (right) on granular diopside aggregate, field of view 7 × 10 mm; (b) bipyramidal crystals of tatarinovite on needles of xonotlite; (c) white massive tatarinovite on grossular, sample size 59 × 53 cm.

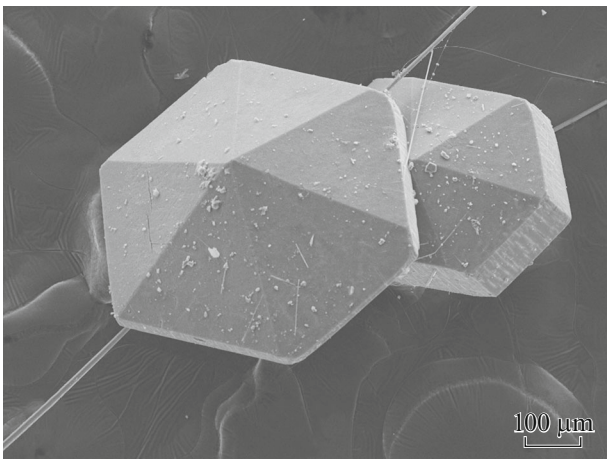

Fig. 3. Secondary electron image of tatarinovite crystals.

octahedra), 501 (O–Si–O bending vibrations of $Si(OH)_6$ octahedra), 417 [O–Al–O bending vibrations of $Al(OH)_6$ octahedra). The bands were assigned according to Miller and Wilkins (1952), Pöllmann et al. (1989), Pushcharovsky et al. (2004), Chukanov et al. (2012), and Pekov et al. (2012).

As can be seen from Fig. 4, the bands of the $B(OH)_4^-$ anions and weak bands of the $B(OH)_3$ molecule are present in the IR spectra of tatarinovite and sturmanite, but are absent in that of thaumasite. It is noteworthy that the presence of both $B(OH)_4^-$ and $B(OH)_3$ in sturmanite was supported by X-ray structure analysis (Pushcharovsky et al., 2004). Characteristic bands of the $Al(OH)_6$ octahedra are also in the IR spectrum of ettringite $Ca_6[Al(OH)_6)_2](SO_4)_3 \cdot 24H_2O$, but are not observed in the IR spectra of EGM, which do not contain Al as a species-defining element, thaumasite, hielscherite, kottenheimite, and buryatite.

CHEMICAL COMPOSITION

Semiquantitative EDS and WDS electron microprobe measurements show the presence of B, Ca, Al, Si, S, and minor Fe in tatarinovite, whereas the contents of the other elements with atomic numbers higher than 8 are below their detection limits. Quantitative electron microprobe measurements were failed because of the mineral instability under electron beam and especially, of its easy dehydration in vacuum for a few minutes (Fig. 5). Tatarinovite is the most unstable in vacuum among all EGM studied by us (i.e. thaumasite, etrringite, sturmanite, buryatite, hielscherite, and kottenheimite).

Quantification of Ca, B, Al, Fe, Si, and S was carried out by the ICP-AES method using a Varian 720-ES spectrometer from 6.05- and 10.29-mg samples. The samples were decomposed by fusion with analytical grade Na_2CO_3 and subsequent dissolution in hydro-

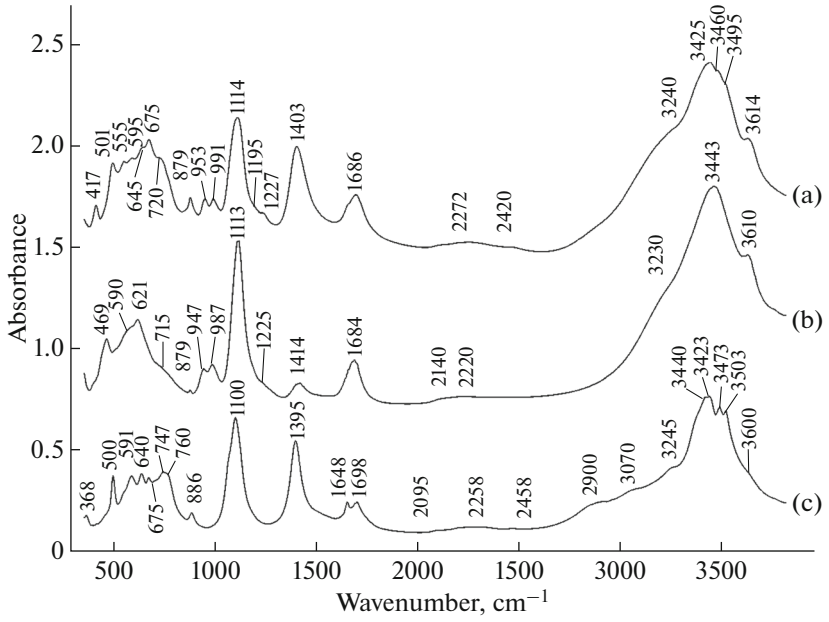

Fig. 4. IR spectra of (a) tatarinovite, (b) sturmanite from Hotazel mine, South Africa, and (c) thaumasite from Uraveli, Georgia.

chloric acid. The spectrometer was calibrated using reference rock samples W-2a, AN, BO-1 (boron ore), and CCB-1, decomposed in a similar way, and certified standard solutions produced by Merck and SPEX; indium was used as an internal standard.

The H_2O content was determined using the Alimarin method involving selective sorption of H_2O on $Mg(ClO_4)_2$ from the gaseous products obtained by ignition of the mineral in an oxygen flow at 1080°C under 1 atm. The CO_2 content was determined using selective sorption on askarite (asbestiform material saturated with NaOH) from gaseous products released upon ignition of tatarinovite under the same conditions (two analyses were performed).

The quantitative chemical composition of the mineral is given in Table 1. The empirical formula of tatarinovite calculated based on 3 Ca apfu is $H_{31.41}Ca_{3.00}(Al_{0.76}Si_{0.25})_{\Sigma 1.01}(B_{0.72}S_{0.65}C_{0.59})_{\Sigma 1.96}O_{24.55}$. This calculation basis was chosen because all sites of the other constituents in the mineral structure are mixed-occupied and/or partly vacant. The correctness of this basis is supported by the density calculated with this formula, which is close to the measured density, as well as by very low Gladstone–Dale compatibility indices –0.13 "superior" and –0.006 "superior" for the calculated and measured density, respectively.

Taking into account the X-ray structure data (see below), the idealized formula of tatarinovite could be written as $Ca_3Al(SO_4)[B(OH)_4](OH)_6 \cdot 12H_2O$. The contents of the constituents calculated from this formula are as follows, wt %: 26.27 CaO, 5.44 B_2O_3, 7.96 Al_2O_3, 12.50 SO_3, 47.83 H_2O, total is 100.00.

X-RAY CRYSTALLOGRAPHIC DATA

The powder X-ray diffraction data of the new mineral (Table 2) were collected on a Rigaku R-AXIS Rapid II diffractometer equipped with CCD detector (Debye–Scherrer geometry, d = 127.4 mm, CoK_α radiation, voltage 40 kV, current intensity 15 mA, exposure time 15 min). All reflections are well indexed in the hexagonal unit cell with the following parameters refined from the powder X-ray data: a = 11.116 (1), c = 10.626 (5) Å, V = 1137.1(5) Å^3.

The single crystal X-ray data for tatarinovite were collected at room temperature in a full sphere of reciprocal space using a Bruker APEX DUO diffractometer

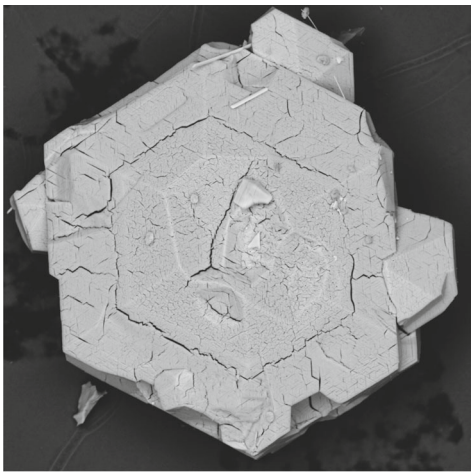

Fig. 5. Partly dehydrated tatarinovite crystal after keeping for several hours in vacuum. Field of view 0.4 × 0.4 mm.

Table 1. Chemical composition of tatarinovite

Component	Average content, wt %	Range of content
CaO	27.40	27.12–27.67
B_2O_3	4.06	4.04–4.07
Al_2O_3	6.34	6.23–6.44
Fe_2O_3	0.03	0.03–0.03
SiO_2	2.43	2.34–2.52
SO_3	8.48	8.46–8.49
CO_2	4.2	3.9–4.5
H_2O	46.1 (2)	
Total	99.04	

equipped with a CCD detector operating with MoK_α-radiation (Table 3). The crystal structure of tatarinovite was solved by direct methods and refined in the SHELX-97 program (Sheldrick, 2008) for 9846 unique reflections with $I > 2\sigma(I)$ (Tables 4–6; Figs. 6–8). The final R factor is 2.52%.

The structure was refined taking into account merohedric twinning. The twinning constituents are present in a ratio of 54 : 46 and linked by the [010/100/00-1] transfer matrix.

The occupancy of the (Al,Si) ite determined at the initial stage of refinement was fixed in the final iteration cycles. In determining the C site occupancies of the carbonate groups C(1) = $C_{0.241(3)}$ and C(2) = $C_{0.302(2)}$, restraints resulting in equal occupancy factors of the sites OC(1) and OC(2), respectively, were used. The refined electron contents for the tetrahedral sites (7.120 for S(1) and 6.448 for S(2); sulfur scattering curve was used in refinement) correspond to the occupancies $S_{0.34}B_{0.33}$ and $S_{0.30}B_{0.34}$ for S(1) and S(2), respectively; occupancy factors of O atoms at the apices of these tetrahedra were restrained to be equal in each tetrahedron. The exception was made only for the OS(21) site with an occupancy factor substantially greater than that of the OS(22) site of the same tetrahedron. Thus, for tetrahedra formed by three atoms OS(21) and one atom OS(22), only the occupancy factor of the OS(22) site was used to calculate the S : B value at the site centering this tetrahedron. The excess oxygen atoms at the OS(21) site made it possible to suggest that they also form a triangle around the additional B site (the S(2)–B distance is 0.57 Å) with an occupancy factor of 0.06 found in the difference synthesis. The positions of hydrogen atoms are found in difference Fourier synthesis and refined in the semi-free mode with O–H distances of 0.86 Å and H···H distances in water molecules ~1.37 Å under the condition of $U_{iso}(H) = 1.2U_{eq}(O)$.

Tatarinovite is a structural analog of thaumasite $Ca_3Si(SO_4)(CO_3)(OH)_6 \cdot 12H_2O$ (Edge and Taylor, 1971; Zemann and Zobetz, 1981; Effenberger et al., 1983; Jacobsen et al., 2003; Martucci and Cruciani, 2006, Gatta et al., 2012). The crystal structure of the new mineral is based on the $[Ca_3(Al,Si)(OH,O)_6(H_2O)_{12}]$ infinite columns running parallel to the c axis and composed of octahedra $[(Al,Si)(OH,O)_6]$ and polyhedra $Ca(OH)_4(H_2O)_4$. Tatarinovite and thaumasite differ in the composition of octahedral M site (with predominant Al or Si, respectively) and additional tetrahedral and triangular anion groups A. In thaumasite, the $[Ca_3(Al)(OH)_6(H_2O)_{12}]$ columns are interconnected by hydrogen bonding with the $[SO_4]^{2-}$ and $[CO_3]^{2-}$ groups, which alternate along the c axis or are completely ordered. The anions $[SO_4]^{2-}$, $[B(OH)_4]^-$, and $[CO_3]^{2-}$ (and impurity $B(OH)_3$ molecules at one of the sites) in tatarinovite are also located between the

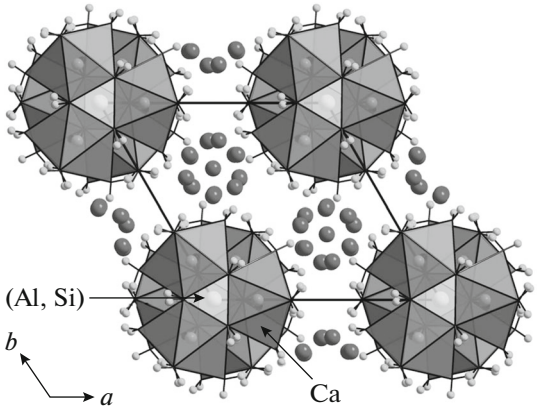

Fig. 6. Crystal structure of tatarinovite. Small circles are H atoms (in water molecules and OH groups); large circles are O atoms of tetrahedral and triangular anion groups. The unit cell is outlined.

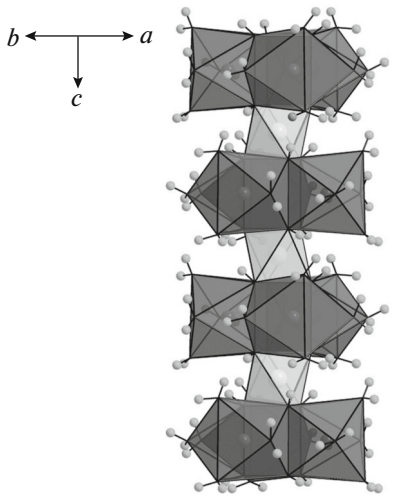

Fig. 7. Column built by (Al,Si)-centered octahedra and Ca-centered eightfold polyhedra in the crystal structure of tatarinovite. Small circles are H atoms.

Table 2. Powder X-ray diffraction data of tatarinovite

I_{obs}	d_{obs}, Å	I_{calc}*	d_{calc}**, Å	*hkl*
100	9.63	100	9.622	100
30	5.556	24	5.556	110
7	4.922	7	4.924	111
3	4.813	2	4.811	200
14	4.654	17	4.652	102
21	3.841	29	3.840	112
1	3.635	1	3.637	210
6	3.567	10	3.567	202
12	3.441	18	3.441	211
5	3.207	8	3.207	300
2	2.988	5	2.987	113
2	2.777	4	2.778	220
10	2.746	23	2.746	302
2	2.665	2	2.669	310
3	2.657	6	2.657	004
5	2.589	11	2.588	131
12	2.538	34	2.538	213
1	2.462	1	2.462	222
2	2.385	4	2.385	312
1	2.324	3	2.326	204
2	2.207	3	2.208	230
9	2.186	26	2.186	223
4	2.164	5	2.161	231
5	2.132	16	2.132	133
1	2.100	2	2.100	410
1	2.060	1	2.060	141
2	2.039	4	2.039	322
1	1.984	2	1.985	115
2	1.953	4	1.953	412
3	1.923	7	1.924	500
1	1.882	1	1.883	134
2	1.834	6	1.835	215
2	1.829	4	1.824	331
2	1.811	2	1.810	502
2	1.792	3	1.792	421
2	1.786	3	1.783	404
1	1.771	2	1.772	006
1	1.747	4	1.749	332
1	1.741	3	1.742	106
1	1.731	2	1.728	510
0.5	1.708	1	1.706	151
0.5	1.688	3	1.688	116
1	1.662	5	1.663	135
2	1.648	8	1.648	144
1	1.605	5	1.604	600
0.5	1.583	1	1.582	430
2	1.565	2	1.565	341
1	1.561	5	1.559	504
1	1.495	1, 4	1.494, 1.494	145, 226
0.5	1.479	1	1.480	522
0.5	1.448	2, 1	1.449, 1.444	154, 343
0.5	1.325	1, 3	1.329, 1.324	008, 261
1	1.294	1, 3	1.294, 1.293	262, 443
0.5	1.240	2	1.239	172
0.5	1.213	3	1.212	630
0.5	1.182	2, 1	1.182, 1.180	362, 346

*For the calculated pattern, only reflections with intensities $I_{calc} \geq 1$ are given. **For the unit cell parameters calculated from single crystal data.

Table 3. Characteristics of tatarinovite crystal and data of single-crystal experiment and structure refinement

Crystal chemical formula	$Ca_3(Al_{0.70}Si_{0.30})\{[SO_4]_{0.34}[B(OH)_4]_{0.33}[CO_3]_{0.24}\}\{[SO_4]_{0.30} \cdot [B(OH)_4]_{0.34}[CO_3]_{0.30}[B(OH)_3]_{0.06}\}(OH_{5.73}O_{0.27}) \cdot 12H_2O$
Weight in terms of formula, amu	615.94
Temperature, K	293(2)
Radiation and its wave length, Å	MoK_α; 0.71073
Symmetry, space group, Z	Hexagonal, $P6_3$; 2
Unit cell parameters	a = 11.1110(4) Å, c = 10.6294(6) Å, V = 1136.44(9) Å^3
Absorption coefficient μ, mm^{-1}	0.934
F_{000}	647
Crystal size, mm	0.20 × 0.20 × 0.30
Diffractometer	Bruker APEX DUO (CCD detector)
$\theta_{min}/\theta_{max}$, °	1.92–59.99
Scanning intervals	$-27 \le h \le 21$, $-25 \le k \le 27$, $-25 \le l \le 25$
Number of reflections	130955
Number of unique reflections	11454 (R_{int} = 0.0302)
Number of unique reflections with $I > 2\sigma(I)$	9846
Software package for data processing	CrysAlisPro, version 1.171.36.32 (Agilent, 2013)
Mode of absorption correction	Multiscan (empirical method using spherical harmonics and algorithm SCALE3 ABSPACK)
Refinement method	Least squares method on F^2
Number of refined parameters	152
$R1$	0.0252 (for reflections with $I > 2\sigma(I)$), 0.0320 (for all reflections)
$wR2$	0.0640 (for reflections with $I > 2\sigma(I)$), 0.0672 (for all reflections)
GoF	1.100
$\Delta\rho_{max/min}$, e/Å^3	0.593/–0.511

$R1 = \rho\|F_o| - |F_c\|/\Sigma|F_o|$; $wR2 = \Sigma w(|F_o|^2 - |F_c|^2)^2/\Sigma w|F_o|^2)^{1/2}$; $w = 1/[\sigma^2(F_o^2) + (0.0316P)^2 + 0.0573P]$; $P = [\max(F_o^2) + 2F_c^2]/3$.

columns and linked to them by the system of hydrogen bonds (Table 6), but they are strongly disordered (Fig. 8). The position occupied by S atom in thaumasite is mixed-occupied in tatarinovite: (S,B,C) with a ratio of S : B : C = 0.34 : 0.33 : 0.24. The S and B atoms are coordinated by oxygen atoms OS(11), OS(12)/OS(13), and OS(14) forming apices of two tetrahedra with different orientation. The C(1) carbon atom is coordinated by the oxygen atoms of the OC(1) site. The site occupied by the C atom in thaumasite is also statically occupied by S, B, and C in tatarinovite, but with a slightly different ratio S : B : C = 0.30 : 0.34 : 0.30. The S and B atoms are coordinated by the oxygen atoms OS(21), OS(22)/OS(23), and OS(24) forming the apices of two differently oriented tetrahedra, while the carbon atom C(2) is coordinated by the oxygen atoms OC(2). The weak maximum in the difference Fourier synthesis was referred to the boron atom with coordination number 3 and coordinated by OH groups occupying the same site OS(21) as the oxygen atoms making up the base of the (S,B)-centered tetrahedron. In should be noted that triangular $B(OH)_3$ molecules were previously identified in the other B-bearing EGM sturmanite (Pushcharovsky et al., 2004).

DISCUSSION

Tatarinovite is the third, after datolite (Varlakov and Polyakov, 1986) and kasatkinite (Pekov et al., 2013), boron mineral to be found in rhodingites of the Bazhenovskoe deposit. Enrichment in boron, displayed as szaibelyite in serpentinite (Sokolov and

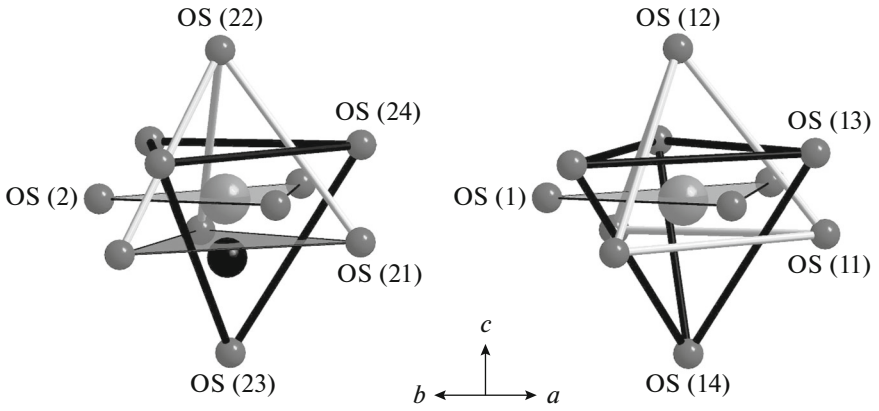

Fig. 8. Arrangement of tetrahedral and triangular groups in the crystal structure of tatarinovite. Large gray spheres are sites S(1)/C(1) (right) and S(2)/C(2) (left). Black sphere depicts additional B site near the S(2) site.

Table 4. Atomic coordinates, equivalent/isotropic thermal displacement parameters (U_{eq}/U_{iso}, Å^2) and Wyckoff positions for tatarinovite

Site	*x*	*y*	*z*	U_{eq}/U_{iso}	Wyckoff positions
Ca	0.194710(12)	0.99864(2)	0.25024(5)	0.01410(1)	6*c*
O(1)	0.13313(9)	0.13063(9)	0.10800(4)	0.01536(10)	6*c*
H(1)	0.1893	0.1981	0.0620	0.018*	6*c*
O(2)	0.13290(9)	0.13140(8)	0.39194(5)	0.01441(9)	6*c*
H(2)	0.2157	0.1844	0.4169	0.017*	6*c*
Ow(1)	0.40320(10)	0.25216(11)	0.25156(15)	0.03389(19)	6*c*
H(11)	0.3875	0.3176	0.2694	0.041*	6*c*
H(12)	0.4829	0.2865	0.2176	0.041*	6*c*
Ow(2)	0.25532(10)	0.40627(9)	0.24911(16)	0.03404(19)	6*c*
H(21)	0.3173	0.4581	0.3017	0.041*	6*c*
H(22)	0.2803	0.4414	0.1762	0.041*	6*c*
Ow(3)	0.00126(12)	0.33811(11)	0.07623(9)	0.02664(13)	6*c*
H(31)	−0.0583	0.3645	0.0828	0.032*	6*c*
H(32)	0.0516	0.3783	0.0124	0.032*	6*c*
Ow(4)	0.00374(14)	0.34733(12)	0.41560(10)	0.0389(3)	6*c*
H(41)	0.0739	0.4202	0.4438	0.047*	6*c*
H(42)	−0.0688	0.3491	0.4379	0.047*	6*c*
$^{Al}0.70^{Si}0.30$	0	0	0.00040(7)	0.01028(2)	2*a*
$S(1) = S_{0.34}B_{0.33}$	1/3	2/3	0.99782(14)	0.0169(2)	2*b*
$C(1) = C_{0.241(3)}$	1/3	2/3	0.99782(14)	0.0169(2)	2*b*
$OC(1) = O_{0.241(3)}$	0.7366(6)	0.2625(6)	0.5025(5)	0.0229(6)	6*c*
$OS(11) = O_{0.295(4)}$	0.6156(3)	0.1915(4)	0.4622(3)	0.0204(6)	6*c*
$OS(12) = O_{0.295(4)}$	1/3	2/3	0.1385(4)	0.0274(13)	2*b*
$OS(13) = O_{0.376(4)}$	0.1905(2)	0.6198(3)	0.0418(3)	0.0253(6)	6*c*
$OS(14) = O_{0.376(4)}$	1/3	2/3	0.8557(3)	0.0175(5)	2*b*
$S(2) = S_{0.30}B_{0.34}$	1/3	2/3	0.50113(15)	0.0176(2)	2*b*
$B = B_{0.06}$	1/3	2/3	0.447(2)	0.015(2)*	2*b*
$C(2) = C_{0.302(2)}$	1/3	2/3	0.50113(15)	0.0176(2)	6*c*
$OC(2) = O_{0.302(2)}$	0.4629(3)	0.7364(5)	0.5040(5)	0.0297(6)	6*c*
$OS(21) = O_{0.458(4)}$	0.1909(3)	0.6174(3)	0.4611(3)	0.0380(7)	6*c*
$OS(22) = O_{0.399(12)}$	1/3	2/3	0.6391(7)	0.095(5)	2*b*
$OS(23) = O_{0.240(4)}$	1/3	2/3	0.3588(6)	0.0279(16)	2*b*
$OS(24) = O_{0.240(4)}$	0.3780(6)	0.8045(5)	0.5465(4)	0.0313(11)	6*c*

*U_{iso}. B (distance S(2)–B 0.57 Å) localized from difference synthesis and with occupancy coefficient 0.06.

Table 5. Selected interatomic distances (Å) in structure of tatarinovite

Ca–Ow(4)	2.4229(9)	S(1)–OS(13)	1.477(2)×3
–O(1)	2.4307(10)	–OS(14)	1.510(3)
–Ow(3)	2.4318(10)	C(1)–OC(1)	1.356(3)×3
–O(2)	2.4349(10)	S(2)–OS(21)	1.456(3)×3
–O(2)	2.4435(11)	–OS(22)	1.467(7)
–O(1)	2.4541(10)	S(2)–OS(24)	1.437(5)×3
–Ow(1)	2.6030(10)	–OS(23)	1.513(6)
–Ow(2)	2.6129(9)		
(Al,Si)–O(1)	0.8590(9)×3	C(2)–OC(2)	1.249(3)×3
–O(2)	1.8669(9)×3		
S(1)–OS(11)	1.433(4)×3	B–OS(21)	1.400(4)×3
–OS(12)	1.496(5)		

Luzin, 1981), tourmaline in talc–carbonate rock, and calcium borosilicates in rhodingites, is characteristic of this locality. The boron specialization of metasomatic assemblages at the Bazhenovskoe deposit is related to the fluid impact of granite that intruded the deposit district (Erokhin and Shagalov, 1998). The identification of tatarinovite unambiguously indicates that part of the boron remains mobile down to the lowest temperatures at which late hydrothermal assemblages are formed within the cavities in rhodingites.

EGM have a pronounced affinity to boron. The cases, when the minerals of this group are the main carriers of boron in the low-temperature hydrothermal paragenetic assemblages are known, the examples being sturmanite from manganese deposits in Cape Province, South Africa; charlesite from the Franklin

Table 6. Hydrogen bonding in tatarinovite

D–H···*A*	*d*(*D*–H)	*d*(H···*A*)	∠*D*–H···*A*	d(*D*···*A*)
O(1)–H(1)···Ow(4)[a]	0.85	2.30	3.1328(14)	167.3
O(2)–H(2)···Ow(3)[b]	0.85	2.30	3.0070(12)	141.0
Ow(1)–H(11)···Ow(2)	0.85	2.15	2.9063(8)	148.1
Ow(1)–H(12)···OS(22)[c]		2.02	2.859(3)	169.8
Ow(1)–H(12)···OS(24)[d]	0.85	*2.08*	*2.764(5)*	*137.1*
Ow(1)–H(12)···OC(2)[c]		*2.39*	*2.994(6)*	*128.1*
Ow(1)–H(12···OS(14)[c]		2.35	2.8230(15)	115.3
Ow(2)–H(21)···OS(21)[e]		2.03	2.811(4)	153.0
Ow(2)–H(21)···OS(23)	0.85	*2.31*	*2.824(3)*	118.8
Ow(2)–H(21)···OC(2)[f]		*2.46*	*3.034(5)*	125.3
Ow(2)–H(22)···OS(13)[e]		1.93	2.754(3)	161.6
Ow(2)–H(22)···OC(1)[g]	0.85	*2.12*	*2.922(5)*	*156.2*
Ow(2)–H(22)···OS(12)		*2.30*	*2.828(2)*	*120.3*
Ow(3)–H(31)···OS(24)[h]		2.00	2.827(6)	164.2
Ow(3)–H(31)···OS(21)[i]	0.85	*2.04*	*2.712(3)*	*134.9*
Ow(3)–H(31)···OC(2)[h]		*2.15*	*2.766(4)*	*129.2*
Ow(3)–H(32)···OS(11)[g]		2.03	2.708(5)	136.5
Ow(3)–H(32)···OC(1)[g]	0.85	*2.09*	*2.709(5)*	*129.7*
Ow(3)–H(32)···OS(13)		*2.35*	*2.787(3)*	*112.1*
Ow(4)–H(41)···OS(24)[e]		1.90	2.728(6)	163.5
Ow(4)–H(41)···OS(21)	0.85	*1.92*	*2.706(3)*	*153.9*
Ow(4)–H(41)···OC(2)[f]		*2.03*	*2.827(4)*	*155.1*
Ow(4)–H(42)···OS(13)[j]		1.91	2.717(3)	158.8
Ow(4)–H(42)···OS(11)[k]	0.85	*1.94*	*2.744(4)*	*157.9*
Ow(4)–H(42)···OC(1)[l]		*2.00*	*2.784(5)*	*153.6*

[a] *y*, –*x* + y, *z* – 1/2; [b] *y*, –*x* + *y*, *z* + 1/2; [c] –*x* + 1, –*y* + 1, *z* – 1/2; [d] *x* – *y* + 1, *x*, *z* – 1/2; [e] –*y* + 1, *x* – *y* + 1, *z*; *f* –*x* + *y*, –*x* + 1, *z*; [g] *y*, –*x* + *y* + 1, *z* – 1/2; [h] *y* – 1, –*x* + *y*, *z* – 1/2; [i] –*x*, –*y* + 1, *z* – 1/2; [j] –*x*, –*y* + 1, *z* + ½; [k] –*y*, *x* – *y*, *z*; [l] *x* – 1, *y*, *z*. Alternative hydrogen bonds are italicized.

Table 7. Comparative data for tatarinovite and other boron members of ettringite group

Mineral	Tatarinovite	Charlesite	Sturmanite	Buryatite	Imayoshiite (IMA 2013-069)
Simplified formula	$Ca_3Al(SO_4)[B(OH)_4]OH)_6 \cdot 12H_2O$	$Ca_6Al_2(SO_4)_2[B(OH)_4] \cdot (OH)_{12} \cdot 26H_2O$	$Ca_6Fe_2^{3+}(SO_4)_2[B(OH)_4] \cdot (OH)_{12} \cdot 25H_2O$	$Ca_6(Si,Fe^{3+})_2(SO_4)_2[B(OH)_4]_2 \cdot (OH,O)_{12} \cdot 24H_2O$	$Ca_3Al(CO_3)[B(OH)_4] \cdot (OH)_6 \cdot 12H_2O$
Crystal system	Hexagonal	Trigonal	Trigonal	Trigonal	Hexagonal
Space group	$P6_3$	$P31c$?	$P31c$	$P31c$?	$P6_3$
a, Å	11.1110	11.16	11.16–11.188	11.14	11.04592(2)
c, Å	10.6294	21.21	21.79–21.91	20.99	10.61502(19)
V, Å^3	1136.44	2288	2350–2375	2256	1121.65(4)
Z	2	2	2	2	2
Strong lines of the powder X-ray diffraction pattern: d, Å (I, %)	9.63 (100)	9.70 (100)	9.67 (100)	9.70 (80)	9.543(100)
	5.556 (30)	5.58 (80)	5.58 (70)	3.85 (60)	4.636(40)
	4.654 (14)	3.855 (80)	3.89 (70)	3.04 (80)	3.822(33)
	3.841 (21)	2.749 (70)	2.774 (50)	2.736 (60)	2.729(31)
	3.441 (12)	2.538 (70)	2.582 (60)	2.596 (100)	2.525(69)
	2.746 (10)	2.193 (70)	2.215 (50)	2.374 (60)	2.174(30)
	2.538 (12)	2.133 (50)	2.161 (40)	2.121 (90)	2.120(23)
				1.498 (70)	1.768(28)
Optical data	Uniaxial (+)	Uniaxial (–)	Uniaxial (+) or(–)	Uniaxial (–)	Uniaxial (–)
	$\omega = 1.475$	$\omega = 1.492$	$\omega = 1.499–1.500$	$\omega = 1.523$	$\omega = 1.497(2)$
	$\varepsilon = 1.496$	$\varepsilon = 1.475$	$\varepsilon = 1.497–1.505$	$\varepsilon = 1.532$	$\varepsilon = 1.470(2)$
Density, g/cm^3	1.79 (meas.)	1.77 (meas.)	1.847 (meas.)	1.895 (calc.)	1.790 (calc.)
	1.777 (calc.)	1.79 (calc.)	1.77—1.855 (calc.)		
Source	This study	Dunn et al., 1983	Peacor et al., 1983; Pushcharovsky et al., 2004	Malinko et al. (2001)	Nishio-Hamane et al., 2015

deposit in New Jersey, United States; and tatarinovite described in this study. At present, five EGM in which boron is the species-defining element are regarded as individual mineral species, whose characteristics are given in Table 7.

Owing to the strong affinity to boron, technogenic analogs of EGM may constitute an increased risk for artifacts from boron-bearing cement materials and concrete: crystallization of these compounds is accompanied by a substantially increasing volume of the solid phase, which can result in breakdown of artifacts and structures (the so-called sulfate attack phenomenon, see Taylor (1997), Terai et al. (2007)). For example, hydrolysis and oxidation of cement materials based on fly ash with a low boron content leads to oxidation of sulfide sulfur to form gypsum (Chervonny et al., 2005a, 2005b). The average content of B_2O_3 in ash of hard and brown coal is 0.08 and 0.13 wt %, respectively; however, fly ashes with much higher B_2O_3 contents are known, for example, 0.38–3.25 wt % in coal ash of the Golubovskaya pit, Donets Coal Basin (Kler et al., 1987), up to 2.34 wt % in coal ash from New Zealand (Yudovich and Ketris, 2005), and up to 0.6 wt % in a sample from the TPP Illinois Power Co. (Cox et al., 1978). Only 50% of boron could be leached from coal ashes. As a rule, the boron concentration in fly ash increases with a decrease in the ash content in the coal. The presence of boron in cement materials based on such an ash could induce the formation of B-bearing phases with the ettringite structure.

ACKNOWLEDGMENTS

Part of this study, the mineralogical characteristics and refinement of the crystal structure, was supported by the Russian Science Foundation (project no. 14-17-00048). Another part, IR spectroscopy and determination of H_2O and CO_2, was supported by the Russian Foundation for Basic Research (project no. 14-05-00190-a). The equipment of the St. Petersburg State University X-ray Diffraction Methods Resource Center was used for the powder X-ray diffraction study. We thank V.O. Yapaskurt for his assistance in scanning electron microscopy of the mineral.

REFERENCES

Antonov, A.A., *Mineralogiya rodingitov Bazhenovskogo giperbazitovogo massiva* (Mineralogy of Rodingites of the Bazhenovsky Ultrabasic Massif), St. Petersburg: Nauka, 2003.

Chervonnyi, A.D., Chukanov, N.V., and Pekov, I.V., Thermal transformations of the SCAS monolith, *Russ. J. Inorg. Chem.*, 2015a, vol. 60, no. 6, pp. 715–723.

Chukanov, N.V., Britvin, S.N., Van, K.V., Mockel, S., and Zadov, A.E., Kottenheimite, $Ca_3Si(SO_4)_2(OH)_6 \cdot 12H_2O$, a new ettringite-group mineral from the Eifel Area, Germany, *Can. Mineral.*, 2012, vol. 50, pp. 55–63.

Cox, J.A., Lundquist, G.L., Przyjazny, A., and Schmulbach, C.D., Leaching of boron from coal ash, *Environ. Sci. Technol.*, 1978, vol. 12, pp. 722–723.

Dunn, P.J., Peacor, D.R., Leavens, P.B., and Baum, J.L., Charlesite, a new mineral of the ettringite group, from Franklin, New Jersey, *Am. Mineral.*, 1983, vol. 68, pp. 1033–1037.

Edge, A. and Taylor, H.F.W., Crystal structure of thaumasite $[Ca_3Si(OH)_6 \cdot 12H_2O](SO_4)(CO_3)$, *Acta Crystallogr.*, 1971, vol. 27, pp. 594–601.

Effenberger, H., Kirfel, A., Will, G., and Zobetz, E., A further refinement of the crystal structure of thaumasite, $Ca_3Si(OH)_6(SO_4)(CO_3) \cdot 12H_2O$, *N. Jb. Miner Mh*, 1983, pp. 60–68.

Efimov, V.I., Rodingites of the Bazhenovskoe chrysotile asbestos deposits, *Ural. Geol. Zh.*, 2004, no. 2, pp. 93–121.

Erokhin, Yu.V. and Shagalov, E.S., Boron-bearing minerals of the Bazhenovskoe deposit resulted from effect of fluids derived from granite intrusion, in *Problemy genezisa magmaticheskikh i metamorficheskikh porod* (Genesis of Igneous and Metamorphic Rocks), St. Petersburg, 1998, pp. 165–166.

Erokhin, Yu.V., Cadastre of mineral species of the Bazhenovskoe deposits, *Materialy Ural'skoi Mineralogicheskoi Shkoly* (Proceedings of the Uralian Mineralogical School), Yekaterinburg: UGGGA, 1997, pp. 178–180.

Gatta, G.D., McIntyre, G.J., Swanson, J.G., and Jacobsen, S.D., Minerals in cement chemistry: a single-crystal neutron diffraction and Raman spectroscopic study of thaumasite, $Ca_3Si(OH)_6(CO_3)(SO_4) \cdot 12H_2O$, *Am. Mineral.*, 2012, vol. 97, pp. 1060–1069.

Granger, M.M. and Protas, J., Determination et étude de la structure cristalline de la jouravskite $Ca_3Mn^{IV}(SO_4)(CO_3)(OH)_6 \cdot 12H_2O$, *Acta Crystallogr.*, 1969, vol. 25, pp. 1943–1951.

Jacobsen, S.D., Smyth, J.R., and Swope, R.J., Thermal expansion of hydrated six-coordinate silicon in thaumasite, $Ca_3Si(OH)_6(CO_3)(SO_4) \cdot 12H_2O$, *Phys. Chem. Miner.*, 2003, vol. 30, pp. 321–329.

Kler, V.R., Volkova, G.A., Gurvich, E.M., et al., *Metallogeniya i geokhimiya uglenosnykh i slants-soderzhashchikh tolshch SSSR: geokhimiya elementov* (Metallogeny and Geochemistry of Coal and Shale-Containing Sequences of the USSR: Geochemistry of Elements), Moscow: Nauka, 1987.

Kusachi, I., Shiraishi, N., Shimada, K., Ohnishi, M., and Kobayashi, S., CO_3-rich charlesite from the Fuka Mine, Okayama Prefecture, Japan, *J. Mineral. Petrol. Sci.*, 2008, vol. 103, pp. 47–51.

Malinko, S.V., Chukanov, N.V., Dubinchuk, V.T., Zadov, A.E., and Koporulina, E.V., Buryatite $Ca_3(Si,Fe^{3+},Al)[SO_4][B(OH)_4]\ (OH)_5O \cdot 12H_2O$, a new mineral., *Zap. Ross. Mineral. O-va*, 2001, vol. 130, pp. 72–78.

Martucci, A. and Cruciani, G., In situ time resolved synchrotron powder diffraction study of thaumasite, *Phys. Chem. Miner.*, 2006, vol. 33, pp. 723–731.

Merlino, S. and Orlandi, P., Carraraite and zaccagnaite, two new minerals from the Carrara marble quarries: their chemical compositions, physical properties, and structural features, *Am. Mineral.*, 2001, vol. 86, pp. 1293–1301.

Miller, F.A. and Wilkins, C.H., Infrared spectra and characteristic frequencies of inorganic ions, *Anal. Chem.*, 1952, vol. 24, pp. 1253–1294.

Mineralogiya rodingitov Bazhenovskogo mestorozhdeniya khrizotil-asbesta (Mineralogy of Rodingites of the Bazhenovskoe Chrysotile–Asbestos Deposit)*, Ivanov, O.K. Spiridonov, E.M. and Krivovichev, V.G.*, Yekaterinburg: UGGA, 1996.

Moore, A.E. and Taylor, H.F.W., Crystal structure of ettringite, *Acta Crystallogr.*, 1970, vol. 26, pp. 386–393.

Nishio-Hamane, D., Ohnishi, M., Momma, K., Shimobayashi, N., Miyawaki, R., Minakawa, T., and Inaba, S., Imayoshiite, $Ca_3Al(CO_3)[B(OH)_4](OH)_6 \cdot 12H_2O$, a new mineral of the ettringite group from Ise City, Mie Prefecture, Japan, *Mineral. Mag.*, 2015, vol. 79, pp. 413–423.

Peacor, D.R., Dunn, P.J., and Duggan, M., Sturmanite, a ferric iron, boron analogue of ettringite, *Can. Mineral.*, 1983, vol. 21, pp. 705–709.

Pekov, I.V., Chukanov, N.V., Filinchuk, Ya.E., Zadov, A.E., Kononkova, N.N., Epanchintsev, S.G., Kaden, P., Kutzer, A., and Gottlicher, J., Kasatkinite, $Ba_2Ca_8B_5Si_8O_{32}(OH)_3 \cdot 6H_2O$, a new mineral from the Bazhenovskoe deposit, the Central Urals, Russia, *Geol. Ore Deposits*, 2013, vol. 155, no. 7, pp. 549–558

Pekov, I.V., Chukanov, N.V., Britvin, S.N., Kabalov, Yu.K., Gottlicher, J., Yapaskurt, V.O., Zadov, A.E., Krivovichev, S.V., Schuller, W., and Ternes, B., The sulfite anion in ettringite-group minerals: a new mineral species hielscherite, $Ca_3Si(OH)_6(SO_4)(SO_3) \cdot 11H_2O$, and the thaumasite–hielscherite solid-solution series, *Mineral. Mag.*, 2012, vol. 76, pp. 1133–1152.

Pöllmann, H., Kuzel, H.-J., and Wenda, R., Compounds with ettringite structure, *Neues Jahrb. Mineral., Abh.*, 1989, vol. 160, pp. 133–158.

Pushcharovsky, D.Yu., Lebedeva, Yu.S., Zubkova, N.V., Pasero, M., Bellezza, M., Merlino, S., and Chukanov, N.V., Crystal structure of sturmanite, *Can. Mineral.*, 2004, vol. 42, pp. 723–729.

Sheldrick, G.M., (2008): a short history of SHELX, *Acta Crystallogr.*, 2008, vol. A64, pp. 112–122.

Skoblinskaya, N.N., Krasilnikov, K.G., Nikitina, L.V., and Varlamov, V.P., Changes in crystal structure of ettringite on dehydration, *Cement Concrete Res*, 1975, vol. 5, pp. 419–431.

Sokolov, Yu.A. and Luzin, V.P., Boric (asharite) mineralization of serpentinites of the Bazhenovsky chrysotile asbestos deposits, *Izv. Akad. Nauk SSSR, Ser. Geol.*, 1981, no. 9, pp. 133–136.

Taylor, H.F.W., *Cement Cchemistry*, London: Thomas Telford Ltd, 1997.

Terai, T., Mikuni, A., Nakamura, Y., and Ikeda, K., Synthesis of ettringite from portlandite suspensions under various Ca/Al ratio, *Inorg. Mater.*, 2007, vol. 43, pp. 881–886.

Varlakov, A.S. and Polyakov, V.O., Gangue minerals from rodingites of the Bazhenovskoe chrysotile asbestos deposits, in *Materialy k topomineralogii Urala*, (Proceedings of Topomineralogy of the Urals), Sverdlovsk: UNTs AN SSSR, 1986, pp. 71–77.

Yudovich, Ya.E. and Ketris, M.P., *Toksichnye elementy primesi v iskopaemykh uglyakh* (Toxic Trace Elements in Fossil Coals), Yekaterinburg: UrO RAS, 2005.

Zadov, A.E., Chukanov, N.V., Organova, N.I., Kuzmina, I.V., Belakovsky, D.I., Nechai, V.G., Sokolovsky, F.S., and Kuznetsova, O.Yu., Comparative study of rosenhahnite from California and from the Urals. Refinement of the formula, *Zap. Ross. Mineral. O-va*, 2000, vol. 129, no. 2, pp. 85–96.

Zemann, J. and Zobetz, E., Do the carbonate groups in thaumasite have anomalously large deviations from coplanarity?, *Sov. Phys. Crystallogr*, 1981, vol. 26, pp. 689–690.

Zoloev, K.K., Chemyakin, V.I., Shmaina, M.Ya., Medvedeva, T.N., et al., *Bazhenovskoe mestorozhdenie khrizotil-asbesta* (Bazhenovskoe Chrysotile Asbestos Deposit), Moscow: Nedra, 1985.

Translated by I. Baksheev